International Journal of Fluid Machinery and Systems
Vol. 4, No. 1, January-March 2011

DOI: 10.5293/IJFMS.2011.4.1.140
ISSN (Online): 1882-9554

**Original Paper (Invited)**

# Incipient Cavitation in a Bulb Turbine: Model Test and CFD Calculation

**Jörg Necker and Thomas Aschenbrenner**

Voith Hydro Holding GmbH & Co. KG
Alexanderstraße 11, 89522 Heidenheim, Germany
joerg.necker@voith.com, thomas.aschenbrenner@voith.com

**Abstract**

For a certain operating point of a horizontal shaft bulb turbine (i.e. volume flow, net head, blade angle, guide vane angle) the efficiency for different pressure levels (i.e. different Thoma-coefficient σ) is calculated using a commercial Computational Fluid Dynamics (CFD-)-code including two-phase flow and a cavitation model. The results are compared with experimental results achieved at a closed loop test rig for model turbines.

The comparison of the experimentally and numerically obtained efficiency and the visual impression of the cavitation show a good agreement. Especially the drop in efficiency is calculated with satisfying accuracy. This drop in efficiency in combination with the visual impression is of high practical importance since it contributes to determine the admissible cavitation in a bulb-turbine. It is seen that the incipient cavitation in Kaplan type turbines has no major importance in determing this admissible amount of cavitation.

**Keywords**: Bulb turbines, multi-phase cfd, incipient cavitation, admissible cavitation

## 1. Introduction

A bulb-turbine is a double regulated turbine in which the Kaplan runner and the generator are mounted on a horizontal shaft. The shaft bearings and the generator are located in a bulb-housing which is supported by piers and which is completely surrounded by water. A common design of a bulb-turbine is completed by an intake, the guide vanes and the draft tube and is shown in figure 1.

A bulb-turbine is most adequate to be used for large flow rates and low head conditions. These conditions can be found for example in run-of-rivers power plants.

Usually for a Kaplan runner some amount of cavitation is allowed during normal operation in contrast to Francis turbines where none or only slightest amount of cavitation is acceptable. This admissible amount of cavitation on Kaplan runners is mainly owed to the fact that a cavitation-free solution would require a deep setting of the machine causing large civil costs and therefore leading to a non-economical solution.

In general, cavitation has different aspects for a water turbine: depending on the intensity and location, the blades can get damaged, vibration can be induced, the performance can deteriorate, and the discharge through the turbine can change significantly. Especially the drop in performance as a function of the Thoma-number σ is of high importance and can be seen exemplary in figure 2. Since the phenomenon cavitation - to be explicitly distinguished from cavitation *damage* - may occur in horizontal bulb-turbines even in normal operation, there is a strong necessity to predict the cavitation - and, as a consequence, implicitly the drop in performance - as accurate as possible.

Accepted for publication December 21, 2010: Paper number O10058S
Corresponding author: Jörg Necker, Dr.-Ing., joerg.necker@voith.com
This manuscript was presented at the 25th IAHR Symposium on Hydraulic Machinery and Systems, September 20-24, 2010, Politechnica University of Timisoara, Romania .

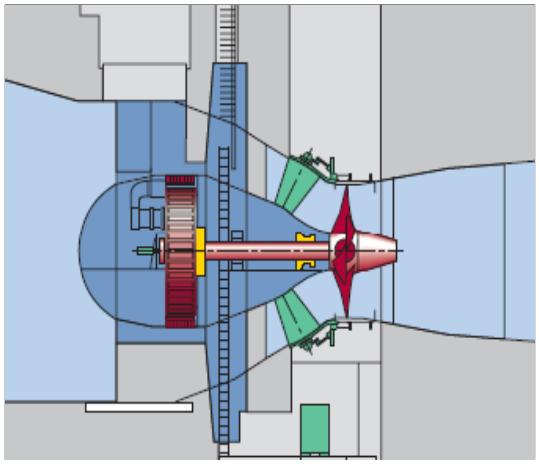

**Fig. 1** Sketch of a bulb turbine

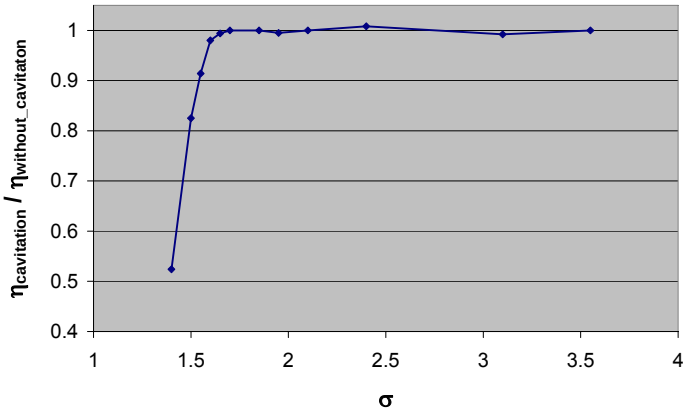


**Fig. 2** Exemplary η-σ-diagram

The admissible amount of cavitation is a difficult decision that has to be done by an experienced engineer and must be governed by the target that the machine runs safe, reliable and without cavitation *damage*. The base for the decision is among others the size and the location of the cavitation, the appearance and the effect on the efficiency. Therefore, cavitation tests as described above with the resulting η-σ−diagram and observation sketches at different Thoma-coefficients are of high practical use. The incipient cavitation - the first cavitation bubble arises in the flow - is difficult to assess in the experiment and leaves always room for discussion. A clear numerical quantitative criteria helps to establish a common understanding. Achieving a first estimation of the cavitation behaviour with appropriate accuracy with numerical methods is desirable since the calculation can be used early in the design phase and different designs can be easily compared. Moreover, the incipient cavitation can be evaluated on a more objective basis.

The prediction of the flow using CFD methods is a challenging task especially for Bulb turbines: there are several sophisticated features in the flow like diffuser flow in the draft tube, small gaps between the runner and the housing, complex three-dimensional unsteady flow in the rotating runner or multi-phase problems like cavitation.

During the last years, CFD has been used routinely within the development process of hydraulic machinery. As a consequence great technological progress could be achieved, the development time of turbines was shortened significantly, and the number of model tests was reduced. A standard procedure today is to compute the flow by applying the Reynolds-averaged Navier-Stokes equations (RANS) on the steady state flow in the individual components which are coupled by mixing-plane interfaces (sometimes also called stage-interface). This standard approach gives fast turn-around times and is a good engineering tool. However, accuracy is limited.

Especially for flow situations where the imposed simplifications tend to neglect important physical phenomena, a careful validation and calibration of the applied CFD method is essential to use CFD as a valuable design tool. Therefore, for today and the (at least!) near future, model tests of homologous machines are unavoidable.

One important example for bulb turbines, where this calibration is needed due to strong modelling of the physics is the quantification of the influence of cavitation on the hydraulic performance of the turbine. Some results of ongoing work in this field are presented. The evaluation of the incipient cavitation is performed following the idea of Stuparu et al. [1]. The numerical results of single phase and two-phase calculations are compared to the results of model tests. The quality, the relevance for the design process, and the applicability of such calculations are discussed.

## 2. Thoma-coefficient

The cavitation coefficient σ (cavitation number, Thoma coefficient) is used as similarity number to characterize the cavitation of an operation point. It is defined in the IEC 60193, sub-clause 1.3.3.6.6, [2].

Commonly used subscripts in conjunction with the Thoma number σ are described in the following:

**$\sigma_{pl}$ (Plant):**

The value of the Thoma number at the operating conditions of the prototype, $\sigma_{pl,}$ depends mainly on the tail water level and the cavitation reference level. It is calculated using the formula described in IEC 60193 annex M. For bulb-turbines, the reference level can be e.g. the top of the runner (TOR) or the top of the hub (TOH).

**$\sigma_i$ (incipient):**

The value of the Thoma number associated with the beginning of visible runner cavitation usually detected by observation, see [2]. The assessment of $\boldsymbol{\sigma_i}$ is difficult especially for Kaplan turbines since in reality the flow channels of the runner differ slightly from each other (geometry tolerance, blade angle …) causing slightly different cavitation behaviour. Moreover, in bulb and Kaplan turbines, the practical use of the incipient cavitation is small since a certain amount of cavitation is allowed even in normal operation due to economical restrictions.

**$\sigma_S$ (Standard)**

The value of $\sigma_s$ was used in the old IEC 193/193A. In the new IEC Code, 60193, this coefficient is not defined anymore. But even today this value is often used for cavitation guarantees. $\sigma_S$ is the theoretical value which is derived from the intersection of two (theoretical) lines: firstly, the horizontal line representing the value without cavitation and, secondly, the approximated line

defined by measurements where the efficiency decreases fast. In some cases, the shape of the η-σ-break curve is such that this Thoma number is difficult to define, see Fig. 3.

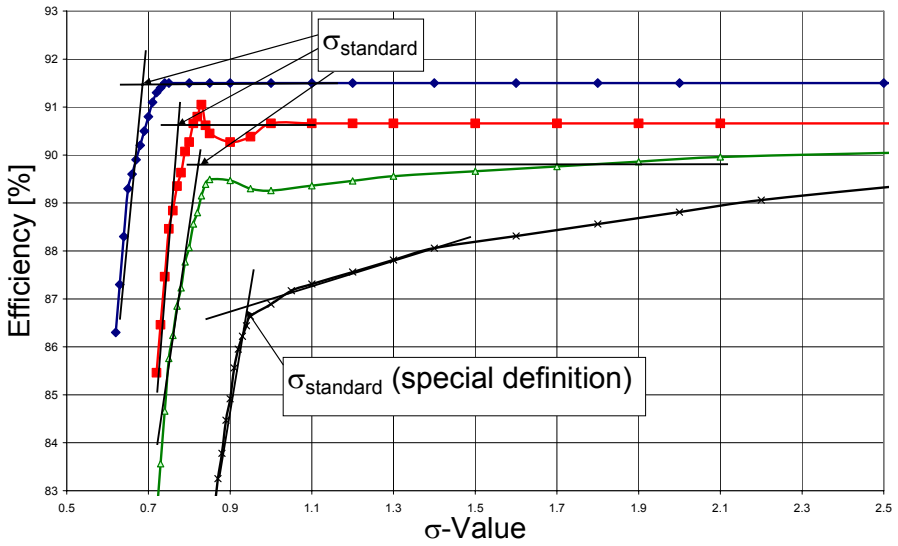


**Fig. 3** Definition of $\sigma_S$

**$\sigma_{adm}$ (admissible)**

As described above, some amount of cavitation is allowed in Bulb-turbines due to economical reasons. The admissible amount of cavitation must be defined by the supplier to guarantee a safe and reliable operation of the machine. Below this $\sigma_{adm}$ the continous operation will lead to severe damage of the machine (e.g. heavy erosion of the blade) or even destruction.

## 3. Experimental set up

The model tests were conducted on the low pressure test rig in the Voith Hydro laboratory in Germany, [3]. The test rig is especially designed for low head machines like bulb- or vertical Kaplan-turbines. The main components are the circuit pump, the head and tail water tanks, and the model turbine driving a motor-generator. They are depicted in figure 4 except of the circuit pump through which the tail and the head water tank are connected.

For the quantitative analysis of the machine, basic physical quantities are measured: pressure, forces, speed, temperature, [4]. The static pressures at the high pressure side is measured in the intake, upstream of the runner while the pressure at the low pressure side $p_S$ is measured at the end of the draft tube. The net head is obtained using the pressure difference and the averaged velocities at the two measuring planes. Measuring the torque via force and well known lever arm, the speed of the runner, the volume flow with an electro-magnetic flow meter and using the evaluated net head, the efficiency of the runner can be evaluated.

The pressure level of the test rig can be changed by changing the absolute pressure in the tail water tank. By evacuating or filling air into the dome of the tail water tank, different suction heads $h_s$ i.e. different Thoma coefficients can be adjusted. The speed of the turbine is usually kept constant.

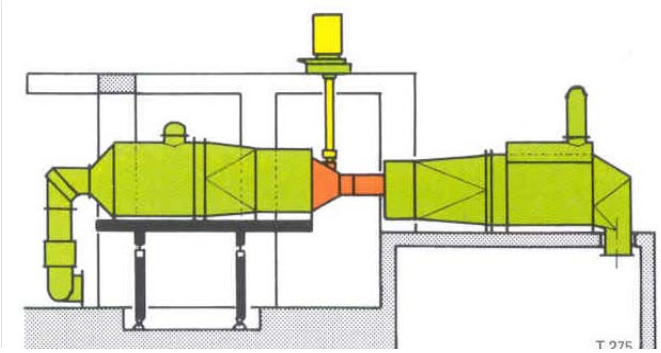

**Fig. 4** Sketch of test rig

The sigma value can be calculated with the measured pressures according to

$$\sigma = \frac{\left(p_{amb} - p_{va}\right)/\rho \cdot g - h_s}{H}$$

The density and the vapour pressure are concluded from the measured temperature of the water. The ambient pressure is measured. The suction head $h_S$ is obtained from the measured low pressure $p_S$ and the correction head between the reference level of the pressure manometer and the pressure tabs in the model.

The experimental uncertainty is for the tested arrangement 0.28 %, see Necker [6].

## 4. Numerical Model

The CFD-code used for the calculations is the commercial software CFX 11.0 and 12.1 of Ansys, [5]. In CFX, the three-dimensional Reynolds-Averaged Navier-Stokes (RANS) equations are solved in conservative form on structured multi-block grids. A finite volume based discretisation scheme is used which is up to second order accurate for the convective fluxes and truly second order accurate for the diffusive fluxes. Time dependent computations can be performed with a second order accurate time stepping scheme. A turbulence model is needed to close the equation system which results from the Reynolds-averaging. A variety of different turbulence models can be applied depending on the application. Here, the SST - model (Menter [9]) was used which

takes advantage of the strength of the k-ε– (free-flow) and the k-ω–model (close to wall). The turbulence model is still one of the largest error sources in modern CFD. However, methods with less or even no modeling are even nowadays not applicable on technical problems, so that the shortly described RANS is the state-of-the-art for the simulation of complex, three dimensional flows.

The calculations are done in stationary mode. The calculation domain consists of the two components guide-vane and runner. It begins upstream of the guide-vanes and ends below the runner, see figure 5. Periodicity in the runner and the guide-vane domains are used. The two components are coupled with a general grid interface with circumferential averaging (stage interface). In the runner domain, the gaps between runner tip and the housing and between the runner and the hub are included in the model. The results of a grid sensitivity study were used (Mohrenberg [9]) to work with a reasonable grid-density. The number of cells used in the guide-vane domain is 260000 nodes and in the runner domain 610000 nodes with refinement towards the walls, resulting in an average y+-value of 95. This relatively large average number is mainly caused by the gap-flow, where the resolution is quite rough compared to the extremely high velocities. Close to the wall, the scalable wall-function of Ansys is used.

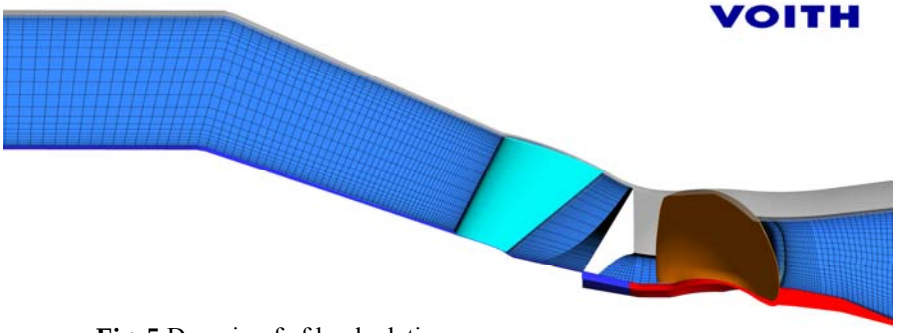


**Fig. 5** Domain of cfd-calculation

The cavitation is modelled with a homogenous multi-phase model that is based on the Rayleigh-Plesset equation for bubble-growth. The equations for the mass-transfer are

$$S_v = \begin{cases} F_{vap}\dfrac{3\cdot r_{nuc}(1-r_v)\rho_v}{R}\sqrt{\dfrac{2}{3}\cdot\dfrac{p_{va}-p_\infty}{\rho_l}}\Bigg|_{p_\infty < p_{va}} \\ -F_{cond}\dfrac{3\cdot r_v\cdot\rho_v}{R}\sqrt{\dfrac{2}{3}\cdot\dfrac{p_\infty-p_{va}}{\rho_l}}\Bigg|_{p_\infty > p_{va}} \end{cases}$$

with $r_v$ as the volume fraction vapour, $r_{nuc}$ as the volume fraction of the nuclei, R as the initial radius of the nuclei, and $F_{vap}$ and $F_{cond}$ as empirical constants. The derivation and the parameters in this model are extensively discussed in Stoltz [6] and Bakir et al. [8]. For the presented calculations, the standard parameters are taken as proposed by Ansys ($F_{cond}$ = 0.01, $F_{vap}$=50, $r_{nuc}$=5e-4).

Initialized by a single-phase calculation, the two-phase calculations are started with different static pressures $p_S$ at the outlet of the domain. For a given static pressure at the outlet, the corresponding σ can be calculated according to

$$\sigma = \frac{\left(p_{amb} - p_{va} + p_S^*\right)\Big/\rho\cdot g}{H}$$

For a better comparison with the experiment, the static pressure at the outlet of the runner domain has to be transferred to the static pressure at the measuring plane of the experimental configuration. This was done with an additional CFD-calculation extending the so far described domain by the draft tube. The static pressure increase between the outlet of the runner and the measuring plane in the draft tube resulted to be approximately 35.4 kPa. A simple check with Bernoulli verified the order of magnitude of the result (34.8 kPa).

An operating point close to the rated point (in this case maximum power and maximum discharge at the rated head) was chosen for the calculation. As physical boundary condition the same mass flow as in the experiment was described for all operation conditions. The $\sigma_{pl,TOH}$ for this head and this machine setting is 2.25 and the $\sigma_{pl,TOR}$ is 2.11. The following 12 sigma-values were adjusted with different pressure levels at the outlet:

**Table 1 In CFD-calculation considered σ-values**

| | | | | | |
|---|---|---|---|---|---|
| ∞ | 2.272 | 2.113 | 1.954 | 1.875 | 1.835 |
| 1.795 | 1.716 | 1.636 | 1.478 | 1.319 | 1.160 |

In a second series of calculations the mass flow was varied for the calculation with the sigma-value of 1.478. This was driven by the measurements which showed a small increase of the model volume flow from 0.873 $m^3/s$ for large sigma values to 0.879 $m^3/s$ for σ=1.4585. The following 5 volume flows were considered: 0.873, 0.879, 0.885, 0.887, and 0.889 $m^3/s$. Larger volume flows caused numerical stability problems.

## 5. Results

For each CFD-calculation the relative hydraulic loss of the runner is evaluated. The absolute loss is calculated as the total pressure difference on a plane upstream and downstream of the runner and referred to the rated head (figure 6).

$$\zeta_{abs} = \frac{\left(\overline{p_{tot,1}} - \overline{p_{tot,2}}\right)}{\rho \cdot g \cdot H_{rated}}$$

with $\overline{p_{tot,1/2}}$ as the mass flow averaged total pressure at plane 1 and 2.

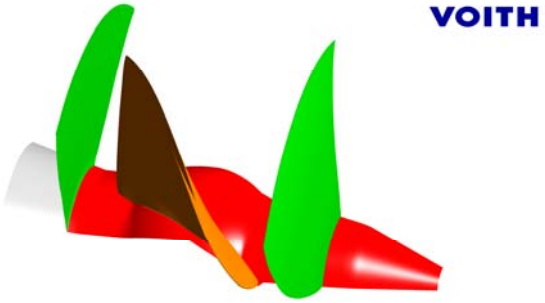


**Fig. 6** Evaluation planes (green) in the runner domain

The relative loss of a certain operation point for the CFD-calculation is defined as the difference of the absolute loss with the highest σ and the absolute loss of the considered operation point:

$$\zeta_{rel} = \zeta_{abs}\big|_{\sigma-high} - \zeta_{abs}\big|_{\sigma}$$

As mentioned above, the experiment delivers the hydraulic efficiency of the model turbine including the losses of the intake, wicket gates, runner and draft tube. A direct comparison between CFD and experiment is therefore not possible. The efficiency obtained from the experiment was transferred in a relative loss. The relative loss for the experiment is defined as the difference of the efficiency with the highest σ and the efficiency of the considered operation point:

$$\zeta_{rel} = \eta\big|_{\sigma-high} - \eta\big|_{\sigma}$$

In figure 7, σ versus the relative loss for both, the experiment and the CFD-calculation, is shown. The orange and red markers indicate $\sigma_{pl,TOH}$ and $\sigma_{pl,TOR}$, the red triangle indicates the relative loss for the single phase calculation ($\sigma \rightarrow \infty$).

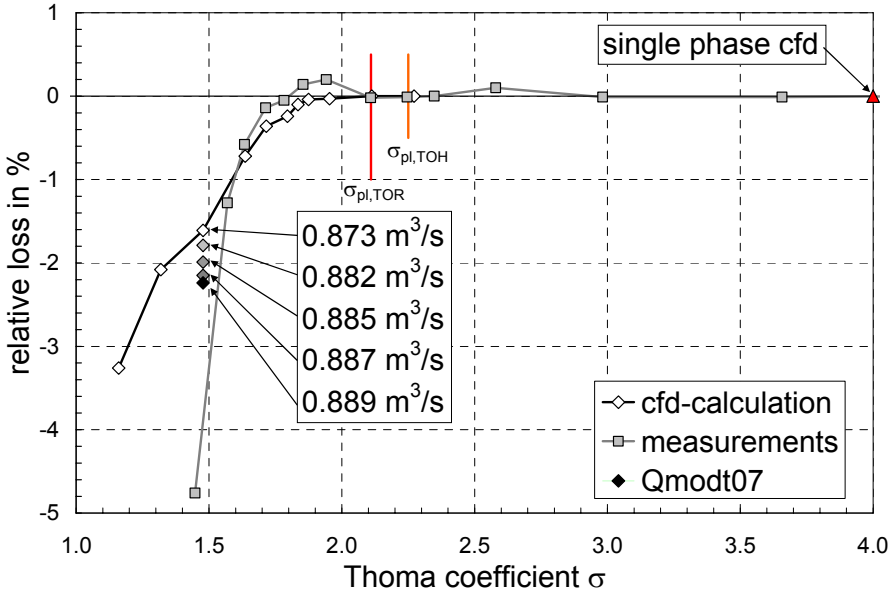


**Fig. 7 Relative loss-σ-curve of the CFD-calculation and the experiment**

From figure 7, the $\sigma_S$-values are obtained according chapter 2 to be $\sigma_{S,\,CFD} \approx 1.79$ and $\sigma_{S,\,Exp.} \approx 1.70$. The results of the second series of calculation with varying volume flow at a constant Thoma coefficient are also included in fig. 7. The volume of the regions affected by cavitation increases with increasing volume flow. It is very sensitive on even small changes in the range of less than 0.3 % of the volume flow. Exemplary pictures in figure 8 show the calculated cavitating region for 0.879 $m^3/s$ (which corresponds to the measured volume flow at σ=1.4585) and 0.889 $m^3/s$ (which corresponds to the calculation closest to the measured efficiency loss).

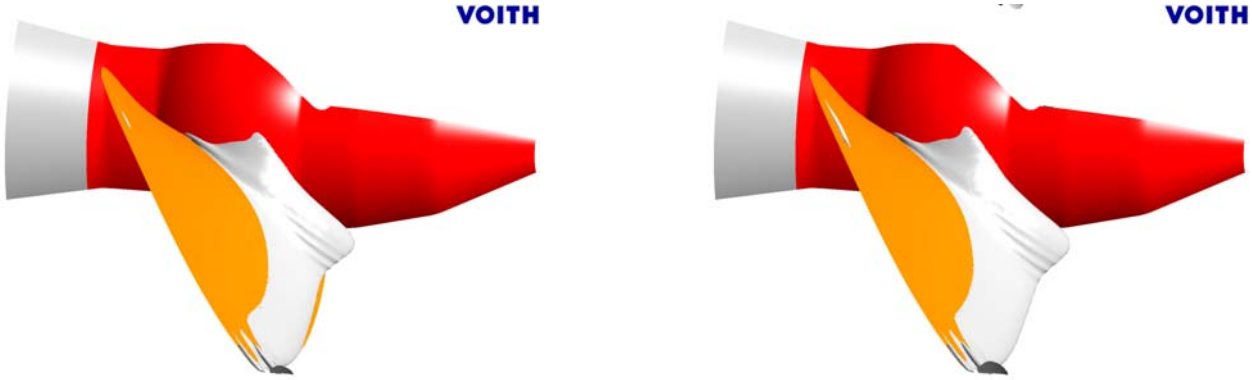


**Fig. 8** Cavitating region at Q=0.873 $m^3/s$ (left) and 0.889 $m^3/s$ (right)

For volume flows larger than 0.889 $m^3/s$ the calculation became unstable caused by an explosive enlargemnet of the cavitating region.

Additionally, visual observations are available from the experiment, see Necker [7]. Detailed sketches are made for the important sigma-values $\sigma_{pl,TOH}$ and $\sigma_{pl,TOR}$. These sketches can be compared with isosurfaces of the volume fraction of water vapour coming from the CFD-calculation. As threshold value for the visibility of the vapour, a vapour fraction of 0.5 is assumed. For some operation conditions with a slightly smaller blade opening (=slightly smaller flow rate) photographs exist of the cavitation bubbles.

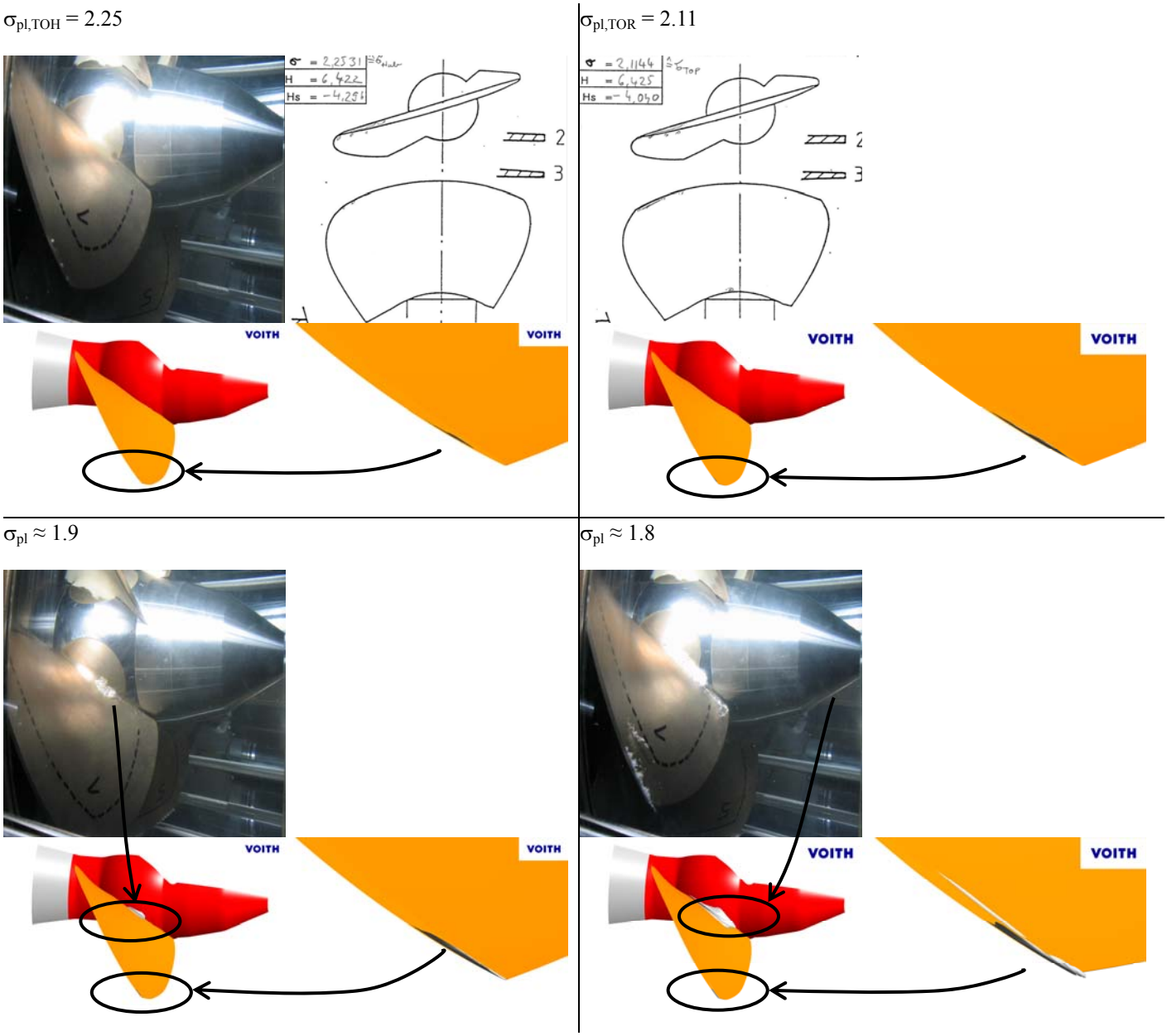


**Fig. 9** Cavitation patterns for different σ at constant volume flow

As an other evaluation - and, as it will be seen in the case of a bulb turbine, it is more a verification of the quality of the results than of practical use for the prototype - the incipient cavitation is derived following a slightly modified approach suggested by Stuparu et al [1]. The idea of this approach is to correlate the Thoma coefficient with the volume of vapour. Defining a certain threshold value of the volume of vapour for "incipient" allows to extra- or interpolate the calculated volumes and to obtain the corresponding Thoma-coefficient. This method introduces objective criteria to determine the inception instead of rather subjective criteria like "first bubble" or even mesh depend criteria like "first cell filled with vapour". Especially for a sensitive event like the transition from liquid water to vapour an objective criteria should be aimed for.

According to Stuparu et al [1] the curve of the volume of vapour can be approximated by a logarthmic equation:

$$\lg V_V = \lg A + B \cdot \sigma$$

Instead of using the absolute volume of vapour as proposed by Stuparu a relative volume of vapour is used. It is calculated by dividing the absolute value by a characteristic volume of the calculation trying to avoid scaling effects. As the characteristic volume is used the volume between the evaluation planes of the domain, see Fig. 6 Evaluation planes (green) in the runner domain. The logarithmic type of the equation is unchanged, only new coefficients are introduced:

$$\lg \overline{V_V} = \lg A^* + B^* \cdot \sigma$$

For the considered operation point the relative volume as a function of the Thoma number is shown in figure 10.

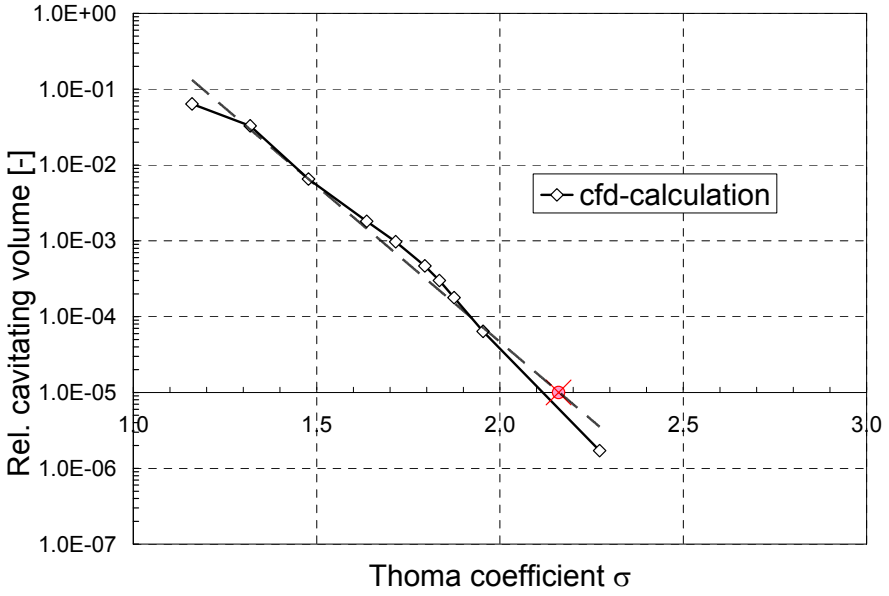


**Fig. 10** Relative cavitation volume vs Thoma coefficient; Incipient Thoma-value

For the incipient cavitation a threshold value of $1.0 \cdot 10^{-5}$ is used resulting in the incipient Thoma-value of approximately 2.16. The coefficients A* and B* are 7780 and -9.471 respectively.

## 6. Discussion

A good consistency within the cfd-calculations is achieved. Comparing the relative result of the single phase calculation with the two-phase calculation including cavitation model at high sigma the difference of the relative loss is less than 0.07 %. This is a confirmation of the standard procedure at Voith to include cavitation models only for those cases in which strong cavitation is expected.

In general, a good prediction of the experimental results - quantitatively and qualitatively - is achieved with the CFD-calculation. The trend of the relative losses is the same and the σ-value of the efficiency drop is less than 5 % off the measured value ($\sigma_S$ = 1.79 vs. $\sigma_S$ = 1.70). Minor differences exist and can be explained by the restrictions of the used cavitation model, the domain and the boundary conditions:

1. The small increase of the measured efficiency comes from a hydraulic profile optimization in a small region caused by the cavitation bubbles. Obviously in these operating conditions, the gas phase and the liquid phase have different velocities. The used cavitation model in the CFD calculation is homogenous, meaning that the gas and the liquid phase have obviously the same velocity. This makes the model inapplicable to predict this profile optimization. Comparing the flow on the blade for σ=2.272 and σ=1.795 shows clearly the flaw of the model: instead of better flow distribution on the blade, the region of disturbed flow is even increased causing increased relative losses. On Fig. the surface streamlines illustrate the disturbed flow region on the suction side close to the hub at the trailing edge.

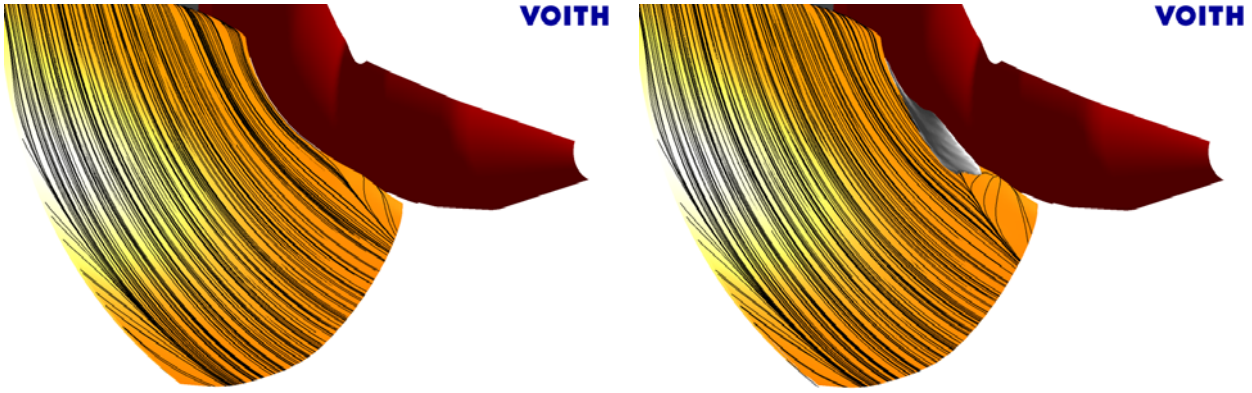


**Fig. 11** Surface streamlines on suction side; left: σ=2.272, right: σ=1.795

The not captured increase of efficiency contributes also to the small difference of the calculated and measured $\sigma_S$-values. If this effect is included artificially by a shift of 0.2 % (maximum efficiency increase of the measurements) of the CFD-results, the excellent consistency of the calculated and measured results between σ = 1.95 and σ = 1.64 can be seen in Fig. . Even the minor dent of the curve at σ = 1.80 is predicted by the CFD-calculation.

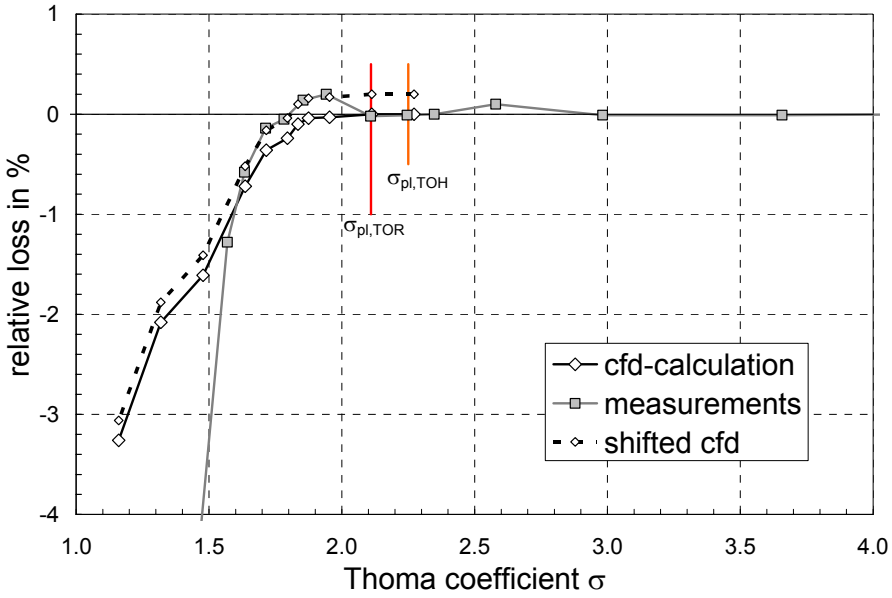


**Fig. 12** Relative loss-σ-curve of the CFD-calculation and the experiment including the shifted CFD results

2. The gradient of the efficiency drop is larger for the measured values than for the calculated ones. In the measurement, the effects of the intake and, especially, the draft tube are included. The cavitation changes the flow-profile entering the draft tube. The losses in the draft tube are very sensitive on these changes. Since the draft tube is not included in the CFD-calculation the changed draft tube performance is obviously excluded of the CFD result.

   Another problem for low σ-values is the fixed boundary condition of the flow rate in the CFD calculation. In reality, the flow rate changes with increased amount of cavitation. This effect was simulated in the second series of calculation. It could be shown that the losses are still underestimated. However, the amount of cavitation and therefore the relative losses are very sensitive on volume changes, e.g. + 0.25 % volume flow causes a loss increase of 0.2 %. The empirical parameters of the cavitation model provided in CFX appear to be conservative in the numerical sense predicting rather smaller than larger cavitating regions, e.g. it was not possible to achieve the measured relative losses before the calculation diverged.

   Beside this, the remark in item 1 would apply also here if the draft tube was also be modeled.

The qualitative results show satisfying agreement between calculation and observation at the test rig. All essential cavitation occurrences at a given σ as well as the size and the location of them are captured. The location of the first cavitation bubbles is detected correctly at the runner tip gap close to the trailing edge. This shows the importance of modeling the gaps for cavitation calculations. Comparing the photograph at $\sigma \approx 1.9$ with the calculation picture shows the correct location and estimated size of the cavitation bubble at the hub. For the lowest given $\sigma \approx 1.8$, even the second streak on the suction side of the blade close to the trailing edge is predicted, however, a little too close to the blade surface and a little too close to the gap.

The evaluation of the incipient cavitation according to the slightly modified approach of Stuparu et al. [1] shows reasonable results, especially with respect to the available model test observations. The model observation at a Thoma-value of 2.25 does not show any cavitation bubbles in the main flow channel while for 2.11 a few bubbles are noted close to the hub, see figure 9. A minor inaccuracy is introduced by the gap cavitation. However, firstly the relative volume of this structure is in the beginning

small compared to the characteristic volume and, secondly, should not be considered at all in Kaplan-type runners for the observation of incipient cavitation. From a practical point of view of a Kaplan-type prototype it can be seen clearly that referring to incipient cavitation conditions lead to unreasonable and non-economical settings of the machine, e.g. for a recently build prototype with safe cavitation behaviour $\sigma_{TOR}$ is in the range of the derived incipient cavitation coefficient. The evaluation of the incipient cavitation in this study was mainly done to demonstrate the quality of the cfd-calculation and to add a correlation of experiments and the approach of Stuparu et al. [1].

In total, the CFD demonstrated to be an important tool in the early design phase. The character of the η-σ-curve is predicted well enough to help the hydraulic designer through the first design iterations. Also, the locations of the regions most prone for cavitation are predicted correctly showing the designer the weaknesses of the current design.

However, for the determination of $\sigma_{adm}$ the information from the CFD-calculation are not precise and not all-embracing enough. For this, the appearance of the cavitation bubbles, the exact position relative to the blade and the stability of the cavitation are highly important on top of the mere size and location. All of this makes the model test inevitable for new designs. Non-modeled parameters like the prototype material or the prototype operation complete the difficult task of defining a σ-value for which a safe and reliable operation of the machine can be guaranteed.

## 7. Conclusion

For a bulb-turbine, experiments on a closed loop test rig as well as a CFD-simulation are performed. The cavitation results are presented quantitatively with the relative losses - σ-diagram and qualitatively with pictures of the CFD-calculation and sketches and photographs of the experimental observation. The Thoma coefficient of incipient cavitation is derived using the approach of Stuparu.

The agreement of the calculated efficiency drop with the measured one is satisfying. The applied cavitation model is inherited not able to predict the observed efficiency overshoot. Correcting in the CFD-results this overshoot artificially the agreement is excellent for moderate cavitation. For a higher amount of cavitation, the prediction deteriorates again because of the missing draft tube in the limited calculation domain and non-physical stiff boundary conditions. Adjusting the volume flow according to model test results revealed a strong sensitivity on the relative losses along with improved results.

The agreement of the calculated pictures and the photographs and sketches of the experimental observation are good. Only for low σ-values (large amount of cavitation), the gap vortex causing a second cavitation structure close to the blade is predicted slightly at the wrong location.

The method applied to determine the incipient cavitation works well for the given parameters. Only the gap cavitation can not be covered which is no disqualification since this kind of cavitation should not be considered for incipient cavitation anyhow. The good agreement with model test results demonstrates also the good quality of the cfd calculation.

In general, the CFD can be seen as a valuable tool in the early design phase with respect to cavitation. An exact determination of operating limits of the prototype (e.g. determination of $\sigma_{adm}$) is, however, beyond the capacity of nowadays CFD-simulations. It is also shown that the incipient cavitation is no design or guarantee criteria of practical use for prototype Kaplan-type turbines.

## Nomenclature

**Latin symbols**

| | | |
|---|---|---|
| A, A*, B, B* | | constants |
| $F_{vap/cond}$ | | empirical constant |
| g | $m/s^2$ | gravitational constant |
| $h_s$ | m | suction head |
| H | m | head |
| $p_{amb}$ | Pa | ambient pressure |
| $p_S/p_S^*$ | Pa | low pressure (suction side) |
| $p_{tot1,2}$ | Pa | total pressure @ plane 1/2 |
| $p_{va}$ | Pa | vapour pressure |
| $p_\infty$ | Pa | free flow pressure |
| $r_{nuc/v}$ | | volume fraction nuclei/vapour |
| R | m | radius nuclei |
| $S_v$ | kg/s | source term evaporation |
| $V_V$ | $m^3$ | volume of vapour |
| $\overline{V_V}$ | | relative volume of vapour |

**Greek symbols**

| | | |
|---|---|---|
| η | % | efficiency |
| ρ | $kg/m^3$ | density |
| σ | | Thoma-coefficient |
| $\sigma_{adm}$ | | Admissible Thoma-coefficient |
| $\sigma_{pl,TOH}$ | | Plant Thoma-coefficient, referred to top of hub |
| $\sigma_{pl,TOR}$ | | Plant Thoma-coefficient, referred to top of runner |
| $\sigma_S$ | | Standard Thoma-coefficient |
| $\zeta_{abs}$ | | absolute loss |
| $\zeta_{rel}$ | | relative loss |

## References


[1] Stuparu, A., Susan-Resiga, R., Anton, L.E., and Muntean, S., 2010, "Numerical investigation of the cavitational behaviour into a storage pump at off desing operating points," IOP Conference Series: Earth and Environmental Science 12, 012068.

[2] International Electrotechnial Commission, 1999, IEC 60193, Second edition.

[3] Sieber, G., Eichler, O., 1984, "Low-pressure circuit test rig (ND) of the 'Brunnenmühle' Hydraulic Research Laboratory," Voith research and construction, Vol. 30.

[4] Brand, F., 1984, “The measuring equipment of the Hydraulic Research Laboratory ‘Brunnenmühle’,” Voith research and construction, Vol. 30.
[5] ANSYS INC, “Ansys CFX,” www.ansys.com/products/fluid-dynamics/cfx/
[6] Stoltz, U., 2007, “Berechnung kavitierender Strömungen in Wasserturbinen,” Diploma thesis, University of Stuttgart.
[7] Necker, J., 2010, “Final model test report, ‘Rio Madeira Santo Antonio Bulb turbine’,” Voith report Nr 4591.
[8] Bakir, F., Rey, R., Gerber, A.G., Belamri, T., and Hutchinson, B., 2004, “Numerical and Experimental Investigations of the Cavitating Behavior of an Inducer,” Int J Rotating Machinery, Vol. 10, pp. 15-25.
[9] Menter, F.R., 1994, “Two-equation eddy-viscosity turbulence models for engineering applications,” AIAA-Journal., 32(8), pp. 1598 - 1605.
[10] Mohrenberg, D., 2008, “Strömungsberechnung in Saugrohren von Francis-Turbinen,” Hochschule Ulm, Fakultät Maschinenbau und Fahrzeugtechnik, Diploma thesis.